18TH WORLD CONFERENCE ON EARTHQUAKE ENGINEERING
WCEE2024
MILAN

MILAN, ITALY
30TH JUNE - 5TH JULY 2024
www.wcee2024.it

AN INDICATOR-BASED MULTI-HAZARD RISK ASSESSMENT FRAMEWORK FOR URBAN-SCALE APPLICATIONS

D. Skoulidou[1]& A.K. Kazantzi[2]

[1] Resilience Guard GmbH, Steinhausen, Switzerland, des.skoulidou@resilienceguard.ch

[2] University of Birmingham, Birmingham, United Kingdom

Abstract: *Owing to the intensified urbanisation and the multiple stressors that are faced by contemporary cities, there is currently an ever-increasing interest for the development of urban-scale risk assessment methodologies targeting a wide spectrum of natural and man-made perils. Representative examples of such perils are the urban flash floods, the urban heat island effect as well as the air quality degradation, whose intensity and frequency have been increasing during the past years due to the adverse consequences of climate change. In this context, the present research offers a practical indicator-based methodology for providing spatially variable risk estimates across a city network that is likely to be affected by a variety of perils. The proposed risk assessment methodology accounts for both the physical and the social risk dimensions, while particular emphasis is given in the definition of the vulnerability component, that involves indicators which account for the susceptibility (i.e., propensity to damage/losses) as well as the lack of capacity to cope. The explicit inclusion of indicators that depict the coping capacities of a city against a certain peril, enables the comparative evaluation of several alternative counter measures within the context of the proposed methodology, on the basis of their ability to reduce vulnerability and ultimately to mitigate risk. The method could be exploited, among others, within the framework of a first-order decision support system to eventually contribute in enhancing urban resilience to future hazardous events. The developed risk assessment framework is demonstrated herein by means of a case study urban-scale application, considering the flash flood peril in the city of Milan.*

1. Introduction

The assessment of risk due to natural and man-made perils in contemporary cities has received lately considerable attention on account of the ever-increasing urbanisation and the accelerated climate change (CC) impacts (IPCC, 2022a). The urban heat island effect, the urban air quality degradation and the devastating flash floods are only some illustrative examples of the aggravated perils that are currently heavily impacting urban environments (UNISDR, 2015). To combat the pertinent direct and cascading adverse consequences, national organisations as well as universities and research institutes, have started developing methodologies for assessing the existing and projected risks in urban areas and consequently proposing efficient measures for mitigating the peril impacts as well as the CC acceleration in an attempt to achieve a more sustainable future for the cities and their occupants (e.g., see Taramelli et al., 2022; Mitoulis et al., 2023).

Among the various methodologies that exist in the literature for evaluating the risk and its components, indicator-based ones are deemed to be among the most efficient when it comes to urban-scale applications. Indicator-based methodologies, are relatively straightforward since they rely on indicators and indices (e.g.,

Leal et al., 2021; Fuchs et al., 2012) in order to identify and quantify the main risk components (e.g., vulnerability) and eventually the risk. For instance, Leal et al. (2021) assessed the physical vulnerability to flash floods of a small study area located within a drainage basin via employing an indicator-based methodology, while Taramelli et al. (2022) employed an indicator-based methodology for assessing the losses in Milan due to an urban flood event. Similarly, an indicator-based vulnerability and risk assessment for the urban heat island in Helsinki was undertaken by Rasanen et al. (2019). In addition to the previous examples, indicator-based methodologies have been also applied in multi hazard risk assessments. For instance, Depietry et al. (2018) applied such a framework in the New York City considering heat waves, inland floods and coastal flooding perils.

In the present study, a simplified indicator-based methodology is developed, that is deemed suitable for urban-scale risk assessment applications accounting for natural and/or manmade perils. The methodology was appropriately structured to enable its seamless integration in a first-order pre-event decision support system (DSS) that aims at providing guidance to decision makers on the effect of alternative risk mitigation actions (Kontopoulos et al., 2023). The next sections define the theoretical framework of the proposed methodology and provide guidelines/directions for all steps that need to be taken, from the selection of the indicators for evaluating the risk components to their normalisation, weighting and aggregation. The developed methodology and its potential are finally demonstrated by means of a case study application which considers the flash flood peril in the city of Milan.

2. Presentation of the methodology

2.1. Definition of risk and its components

In the developed methodology, risk is defined according to IPCC (2022a) as a function of three components: hazard (H), exposure (E) and vulnerability (V) [see Eq.(1)]. Hazard accounts for the intensity and the likelihood/frequency of the peril, exposure accounts for the assets (e.g., people, buildings, infrastructure) that are exposed to the peril and are likely to experience some kind of loss/damage, while vulnerability characterises the predisposition of these assets to be adversely affected by the peril, involving concepts of susceptibility (S) to harm/damage and lack of capacity to cope (COP) [see Eq.(2)] (IPCC, 2022b).

$$\text{Risk}=f(\text{H, E, V}) \quad (1)$$

$$\text{V}=f(\text{S, COP}) \quad (2)$$

Furthermore, in order to account for the multidimensionality of the risk, the social (SO) and the physical (PH) dimensions of the exposure as well as the susceptibility components are identified and treated separately.

2.2. Selection, normalisation and scoring of indicators

For the definition of the three risk components, suitable sets of indicators need to be initially selected. Although, at least for the time being, there exist no specific selection guidelines, some common rules apply, as outlined by Birkmann (2013). The selection of the indicators in the present methodology is performed on the basis of existing literature, field knowledge and/or expert judgement, accounting for the considered peril, the specific characteristics of the investigated area as well as for the data availability.

Following the indicators selection, their normalisation is performed in order to express them in a common scale (i.e., normalised) that will allow their subsequent aggregation. In the proposed methodology, all indicators are normalised such that their value/score ranges from 0 to 1, while their normalisation depends on their nature. Score values equal to 0 denote no susceptibility or complete lack of any capacity to cope, whereas score values equal to 1 denote high susceptibility or high level of capacity to cope.

Quantitative indicators are normalised according to the min-max normalisation formula,

$$x_{Norm,i} = \frac{x_i - x_{min}}{x_{max} - x_{min}} \quad (3)$$

where, x_i is the unnormalised data point of the i^{th} indicator, x_{min} is the minimum value of the i^{th} indicator and x_{max} is the maximum value of the i^{th} indicator. On the other hand, qualitative indicators could be binary (e.g., yes/no) and consequently could be assigned a score equal to either 1 or 0. Non-binary qualitative indicators could be defined by considering a spectrum of options and assign a score to each one of them that ranges between 0 and 1 (based on existing literature evidence and/or expert opinion).

2.3. Aggregation of indicators

Vulnerability component

The vulnerability component comprises three main sub-components and consequently three different kind of vulnerability indicators: (a) the physical susceptibility that essentially quantifies how prone to peril-induced damages is the urban built environment, (b) the social susceptibility that assesses the harm potential of the people exposed to the considered peril and (c) the capacity to cope element that accounts for those characteristics/properties/measures that could contribute in mitigating the physical and social susceptibility.

Following the peril-specific selection and normalisation of the appropriate sets of vulnerability indicators, those are consequently combined, utilising an appropriate aggregation method, to deliver the associated susceptibility/capacity to cope sub-components. The weighted arithmetic average was adopted herein for combining/aggregating the susceptibility and coping capacity indicators to eventually form the three vulnerability sub-components according to the following expressions:

$$\text{Physical susceptibility: } S_{PH} = w_{S_{PH1}} \cdot S_{PH1} + w_{S_{PH2}} \cdot S_{PH2} + \cdots + w_{S_{PHi}} \cdot S_{PHi} \quad (4)$$

$$\text{Social susceptibility: } S_{SO} = w_{S_{SO1}} \cdot S_{SO1} + w_{S_{SO2}} \cdot S_{SO2} + \cdots + w_{S_{SOj}} \cdot S_{SOj} \quad (5)$$

$$\text{Coping capacity: } COP = w_{COP_1} \cdot COP_1 + w_{COP_2} \cdot COP_2 + \cdots + w_{COP_k} \cdot COP_k \quad (6)$$

where, $w_{S_{PHi}}$, $w_{S_{SOj}}$, w_{COP_k} are the weights attributed to the i^{th} indicator expressing physical susceptibility, the j^{th} indicator expressing social susceptibility and the k^{th} indicator expressing the capacity to cope, respectively, and S_{PHi}, S_{SOj} and COP_k are the normalised physical susceptibility, social susceptibility and coping capacity indicators, respectively. The weights assigned to the indicators of each susceptibility dimension need to sum up to 1.0, while the sum of the weights assigned to the indicators of the coping capacity sub-component should be either equal to or lower than 1.0.

In the presented methodology, the vulnerability component is defined via combining the previously presented vulnerability sub-components, i.e., the total susceptibility (physical and social) and the lack of coping capacity (1-COP) according to the following equation:

$$V = (w_{S_{PH}} \cdot S_{PH} + w_{S_{SO}} \cdot S_{SO}) \cdot (1 - \text{COP}) \quad (7)$$

where, $w_{S_{PH}}$ and $w_{S_{SO}}$ are the weights attributed to the physical and social susceptibility dimensions, respectively, which should also add to 1.0.

The inclusion of the capacity to cope as a separate urban vulnerability sub-component is considered a major advantage of the proposed framework, as it provides direct and quantifiable answers to the pertinent authorities (e.g., local or state) as to what can be modified, newly implemented or done differently in order to improve the performance of the city network against different kind of perils and thus fully serves the needs of a risk-aware pre-event DSS. It is also highlighted that the sum of w_{COP_k} in Eq.(6) could be either equal or lower to 1.0, depending on the available measures to mitigate vulnerability as well as their efficiency. A further advantage of the proposed combination rule for estimating the vulnerability component, as reflected in Eq.(7), lies in the addition of the two susceptibility dimensions, i.e., physical and social, that allows for the consideration of each dimension independently and regardless of the existence of the other. By contrast, the aggregation of the total susceptibility with the lack of coping capacity is performed by means of multiplication. The multiplication of the two sub-components allows the vulnerability score to take its maximum value, i.e., equal to the total susceptibility score, in case of complete absence of coping capacity.

Exposure component

Similarly to the procedure adopted in the case of the vulnerability component, the exposure component is also discretised to indicators that account for the physical and the social dimension. Following the selection and the normalisation of the exposure indicators, so as to vary between 0 (to denote no exposure) to 1 (to denote high exposure), those are subsequently aggregated to form the following two exposure sub-components:

$$\text{Physical exposure: } E_{PH} = w_{E_{PH1}} \cdot E_{PH1} + w_{E_{PH2}} \cdot E_{PH2} + \cdots + w_{E_{PHq}} \cdot E_{PHq} \quad (8)$$

$$\text{Social exposure: } E_{SO} = w_{E_{SO1}} \cdot E_{SO1} + w_{E_{SO2}} \cdot E_{SO2} + \cdots + w_{E_{SOr}} \cdot E_{SOr} \quad (9)$$

where, $w_{E_{PHq}}$, $w_{E_{SOr}}$ are the weights attributed to the q^{th} and r^{th} indicators expressing physical exposure and social exposure, respectively, and E_{PHq} and E_{SOr} are the normalised physical exposure and social exposure indicators, respectively. The weights assigned to the indicators of each exposure sub-component should add to 1.0.

The aggregation of the exposure sub-components into the exposure component is performed according to the following combination rule:

$$E = w_{E_{PH}} \cdot E_{PH} + w_{E_{SO}} \cdot E_{SO} \quad (10)$$

where, $w_{E_{PH}}$ and $w_{E_{SO}}$ are the weights assigned to the physical and the social exposure dimension, respectively, adding to 1.0.

Hazard component

The hazard assessment involves the estimation of the probability that a hazardous event of a particular intensity will occur within a specific timeframe at a particular location. In the proposed indicator-based methodology, the score associated with the hazard index *H* is evaluated as per Eq.(11) on account of a considered hazard scenario, as the product of (a) the score assigned to the hazard intensity indicator, *Intensity* (considering low up to extremely high intensities, with higher scores assigned to higher intensities) that accounts for the magnitude of the hazard event (e.g., inundation depths) associated with the said scenario and (b) the score assigned to the likelihood indicator, *Likelihood* (ranging from frequent to very rare, with higher scores assigned to more frequent events) that depicts the mean return period of the considered hazard scenario . Hence, on account of the above the hazard component score for a certain hazard scenario may be evaluated as:

$$H = Intensity \cdot Likelihood \quad (11)$$

The *Likelihood* may be set to one, to either investigate "*what-if*" scenarios or if the performance of the city network is evaluated considering past events (to for instance calibrate the methodology or different risk mitigation measures). In such cases, the likelihood of the event is irrelevant as the event is essentially considered to be deterministic, rather than uncertain.

Risk

The risk score is calculated via aggregating the previously determined vulnerability, exposure and hazard component scores as follows:

$$R = \sqrt[3]{E \cdot V \cdot H} \quad (12)$$

The geometric mean is adopted for the aggregation of the risk components, instead of the arithmetic mean, in order to fulfil the main assumption that complete absence of any one of the risk elements, i.e., vulnerability, exposure or hazard in a certain location, results in zero risk for this location.

2.4. Weighting of indicators

The process of aggregating the indicators to eventually compute a composite index, for e.g., the physical susceptibility, includes also the definition of their weights. According to Papathoma-Kohle et al. (2019) this process is the most sensitive step among those that need to be taken for the computation of the required indices. In the literature, there are currently available several different approaches for computing the indicator weights, such as methods that are based on statistical analysis, e.g., the principal component analysis (PCA) and the factor analysis, methods that are based on expert judgment, e.g., the analytical hierarchy process (AHP) and the budget allocation process, as well as the equal weighting approach. However, no established generic methodology currently exists on how to select the most appropriate weighting scheme. In the case study application of the proposed methodology both equal and unequal weighting approaches will be utilised, as detailed in the following sections.

3. Case study application

3.1. Study area

To showcase the proposed risk assessment methodology, an example application is presented in this section for the case of flash flood in the city of Milan in Italy. Flash floods are sudden local flood events that are characterised by high water volumes and short duration following a heavy precipitation incident. In the past, Milan was affected by several flash flood events and hence in the 70s a number of flood protection measures were implemented in the city (Ravazzani et al., 2016). One such measure is the construction of a bypass channel of the Seveso river, in which the excess discharge is directed (Becciu et al., 2018). However, the recent flood incidents showcased that the capacity of such flood protection measures is often exceeded and hence flood events continue to adversely affect the city, like the one of July 8th, 2014 that resulted in severe economic losses (~55M€ according to Ravazzani et al., 2016).

The spatial resolution to which the risk components scores and consequently risk scores are offered is highly dependent on the resolution of the available data. In the present case study, the Building Block (BB) level spatial resolution is adopted and hence all scores are derived per BB. In the following sections, the three risk components are built-up and their scores are derived for the entire city of Milan using the referred exposure and hazard data that are offered per BB. On that basis, spatially variable estimates of risk scores are first derived and used for the baseline assessment of the city against the flash flood peril, while alternative risk mitigation scenarios are also examined through the implementation of different COPs.

3.2. Vulnerability

The build-up of the vulnerability component in the proposed indicator-based urban risk assessment methodology is demonstrated in this section for the case of flash flood. Table 1 summarises the vulnerability indicators that are proposed for depicting the three dimensions which are considered for this component, i.e., the physical (PH), the social (SO) and the capacity to cope (COP). The susceptibility and capacity to cope scores of the selected indicators that are presented in Table 1 were mainly founded on evidences from existing literature. However, in some cases such scores were not readily available due to the lack of existing pertinent studies (Papathoma-Kohle et al., 2022). In those cases, expert judgement was utilised for the score estimation that might only partially founded on relevant literature that is again provided in Table 1.

Since BB level spatial resolution is adopted in this case study, all indicator scores that are available at a different resolution level need to be transformed into BB scores prior to their aggregation into the vulnerability sub-components. For instance, if an indicator is defined on a city scale, the same score is applied to all BB of the city. The required data for the calculation of the four indicators selected to express physical susceptibility were collected from the Italian National Institute of Statistics.

Table 1. Vulnerability indicators, scores and weights for the peril of flash flooding in Milan, Italy.

Category	Indicator	Score	Weight	Reference
Physical Susceptibility	Construction material (CM)	RC: 0.1 Masonry:0.45 Other:1.0	0.25	Leal et al. (2021); Taramelli et al. (2022); Muller et al. (2011)
	Conservation status (CS)	Excellent:0.1 Good:0.4 Mediocre:0.7 Very bad:1.0	0.25	Kappes et al. (2012); Leal et al. (2021); Taramelli et al. (2022)
	Number of storeys (NS)	One:1.0 Two:0.5 More than two:0.33	0.25	Kappes et al. (2012), Leal et al. (2021)
	Age of construction (AC)	Before 1946: 1.0 1946-1960: 0.75 1961-1980: 0.5 1981-2000: 0.25 After 2001:0.1	0.25	Leal et al. (2021), Taramelli et al. (2022)

Category	Indicator	Score	Weight	Reference
Social Susceptibility	Percentage of older adults 65 and over (Eld65)	Max: 36% Min:0%	0.25	Karagiorgos et al. (2016); Chang et al. (2021). Max based on maximum value for the EU countries according to World Bank (2023b)
	Percentage of children under 15 (Chi15)	Max: 30% Min:0%	0.25	Cutter et al. (2003); Chang et al. (2021); Moreira et al. (2021); Karagiorgos et al. (2016). Max based on maximum value for the EU countries according to World Bank (2023a)
	Unemployment rate (UR)	Max: 41.55% Min:0.0%	0.25	Karagiorgos et al. (2016); Krellenberg and Welz (2017). Max based on maximum value for the EU countries according to World Bank (2023c)
	Education level (EL)	University:0.0 High school:0.25 Lower aver:0.5 Elementary:0.75 W/O education:1.0	0.25	Karagiorgos et al. (2016); Cutter et al. (2003). Scores based on expert judgement
Coping Capacity	Early warning system (ESW)	YES: 1 NO: 0	0.10	Pathak et al. (2020)
	Maintenance of drainage system (DSM)	Frequently: 1.0 Occasionally: 0.5 Scarcely: 0.0	0.20	Expert judgement
	Past experience with major floods (PEF)	Every year: 1.0 Once every 5-10 years: 0.5 Once every 20 years or more: 0.0	0.05	Pathak et al. (2020); Muller et al. (2011); Hidayah et al (2021); Karagiorgos et al. (2016). Scores based on expert judgement.
	Flood protection infrastructure (FPI)	YES: 1 NO: 0	0.40	Bigi et al. (2021). Scores based on expert judgement.
	Percentage of greenery within 100m (PG)	<5: 0.0, >=5&<25: 0.2, >=25&<50: 0.5, >=50&<75: 0.7, >=75: 0.9,	0.20	Kim et al. (2016); Muller et al. (2011). Scores based on expert judgement.
	Awareness on the flood hazard (AFH)	YES: 1 NO: 0	0.05	Karagiorgos et al. (2016); Pathak et al. (2020)

The four selected physical susceptibility indicators, i.e., CM, CS, NS and AC, are aggregated into the physical susceptibility sub-component (S_{PH}) based on the weighted average [see Eq.(4)], where the weights of the indicators (w_{CM}, w_{CS}, w_{NS} and w_{AC}) are assumed to be equal, hence all being set to 0.25. Similarly, the equal weight approach is used for aggregating the selected four social susceptibility indicators, i.e., Eld65, Chi15, UR and EL, into the social susceptibility sub-component (S_{SO}) [see Eq.(5)], with w_{Eld}, w_{Chi}, w_{UR} and w_{EL} being set equal to 0.25. The selected six coping capacity indicators, i.e., EWS, DSM, PEF, FPI, PG and AFH, are aggregated into the coping capacity sub-component (COP) [see Eq.(6)] following an unequal weight approach, with w_{EWS}, w_{DSM}, w_{PEF}, w_{FPI}, w_{PG} and w_{AFH} assigned values equal to 0.10, 0.20, 0.05, 0.40, 0.20 and 0.05, respectively (note that the weights of the considered COPs add to 1 for the case at hand, but this is not a prerequisite). The highest weight, i.e., 0.40, is assigned to FPI, the COP indicator associated with the construction of new code-conforming flood protection infrastructure (or an appropriate enhancement of the capacity of the existing one), as this counter measure is anticipated to have the highest impact on the community and the built environment. The PG and the DSM COP indicators are assigned weights equal to 0.20 each, followed by the EWS that was assigned a weight equal to 0.10. The lowest weights are assigned to the COPs related to PEF and the EFH, i.e., equal to 0.05, since these two COPs are expected to have the lowest impact on the community and no impact on the built environment.

Assuming an equal contribution for the two susceptibility sub-components, i.e., $w_{S_{PH}}$=$w_{S_{SO}}$=0.5, the total susceptibility score per BB is determined and presented in Figure 1a, along with the lack of coping capacity score (1-COP), presented in Figure 1b. Finally, the aggregation of the three vulnerability sub-components into the vulnerability component (V), which represents the BB vulnerability score, is performed according to Eq.(7).

Figure 1c shows the spatial distribution of the vulnerability scores in all BBs of the city of Milan. The relatively low vulnerability scores (<0.5) determined for most parts of the city are attributed to both the moderate inherent total susceptibility (average susceptibility score ~0.6) as well as the several COP indicators already implemented in the city (average lack of coping capacity score ~0.7).

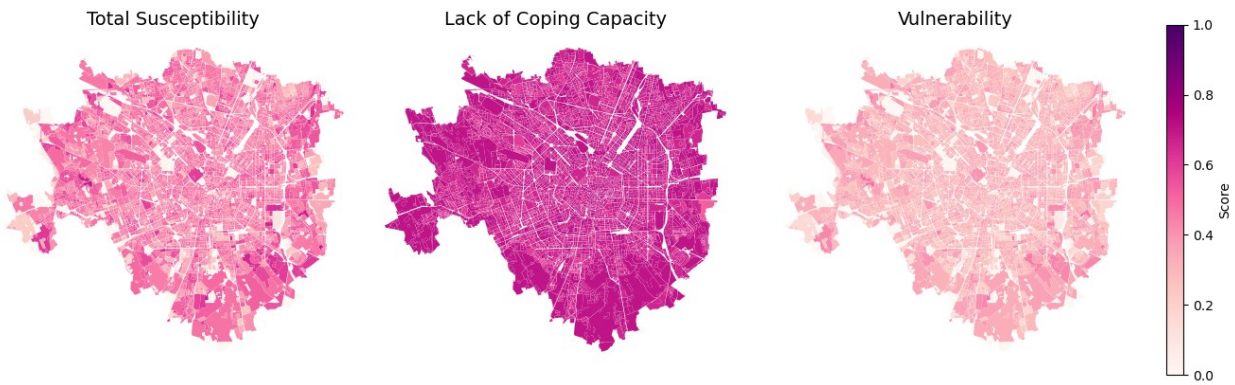

(a) (b) (c)

Figure 1. Spatial distribution of (a) the total susceptibility, (b) the lack of coping capacity, and (c) the vulnerability scores for the city of Milan.

3.3. Exposure

The exposure component of the risk follows a similar approach to that adopted for the vulnerability components and hence, social and physical exposure sub-components, shown in Table 2, are considered separately and are consequently aggregated for defining the exposure component. For the investigated case study, in case of the existence of a critical infrastructure in a BB both the social and the physical exposure scores are set equal to 1.0 (i.e., to the maximum exposure score).

Table 2. Exposure indicators, scores and weights for the peril of flash flooding in Milan, Italy.

Category	Indicator	Score	Weight	Reference
Physical Exposure	Building density	Max:100% Min:0%	0.50	Thouret et al. (2014) Max based on max value according to the Italian Nat. Inst. for Statistics (2023)
Social Exposure	Population density	Max:14.5% Min:0%	0.50	Bigi et al. (2021) Max based on max value according to the Italian Nat. Inst. for Statistics (2023)

Figure 2a and 2b present the spatial variability of the physical and social exposure scores, respectively, accounting for the critical infrastructure. Higher physical exposure scores are observed close to the centre of Milan, reflecting the denser urban fabric of the city centre compared to the surrounding areas, whereas both high and low social exposure scores are scattered across the city without showing any constant trends. All BBs with critical infrastructure obtain the maximum score, i.e., 1, both for the physical and social exposure elements and hence appear in the pertinent figures with dark purple colour.

Following the identification of the exposure indicators, the collection of data and their normalisation, the aggregation of E_{PH} and E_{SO} is performed based on the weighted average and the equal weight assumption [Eq.(10)]. Further to the previously presented effect of the critical infrastructure on the overall exposure, the evaluation of Eq.(10) shows that zero exposure in a BB can be achieved only when both physical and social exposure are equal to zero. The spatial variability of the exposure scores is illustrated in Figure 2c, highlighting that, apart from the BBs that have some kind of critical infrastructure and hence receive by default an exposure score equal to 1, the highest scores are concentrated close to the city centre, in agreement with the spatial distribution of the scores obtained for the two exposure sub-components.

Figure 2. Spatial variability of (a) physical, (b) social and (c) total exposure scores.

3.4. Hazard

For the hazard component of the risk, a probabilistic flash flood hazard assessment is considered for the case study application, that provides the maximum expected inundation depth in the area around the Seveso river considering a 10-year mean return period. In order to translate the referred data into BB hazard scores, the inundation depths that are encountered within each BB block are initially averaged and a mean inundation depth is evaluated per BB. Figure 3a (and Figure 3b in enlarged view) shows the spatial distribution of the mean inundation depth of the considered flash flood scenario expressed in a BB resolution level. Those BBs that are not affected by the considered flash flood hazard scenario appear in Figure 3 in light grey colour. Next, the inundation depths are translated into hazard scores according to Table 3 and Eq.(11), using i=1, given that only one return period was accounted for, and a likelihood score equal to 1, essentially implying that the considered hazard scenario is extremely likely to affect in the near future the area of interest. The spatial distribution of the flash flood hazard scores in the affected area is illustrated in Figure 3c.

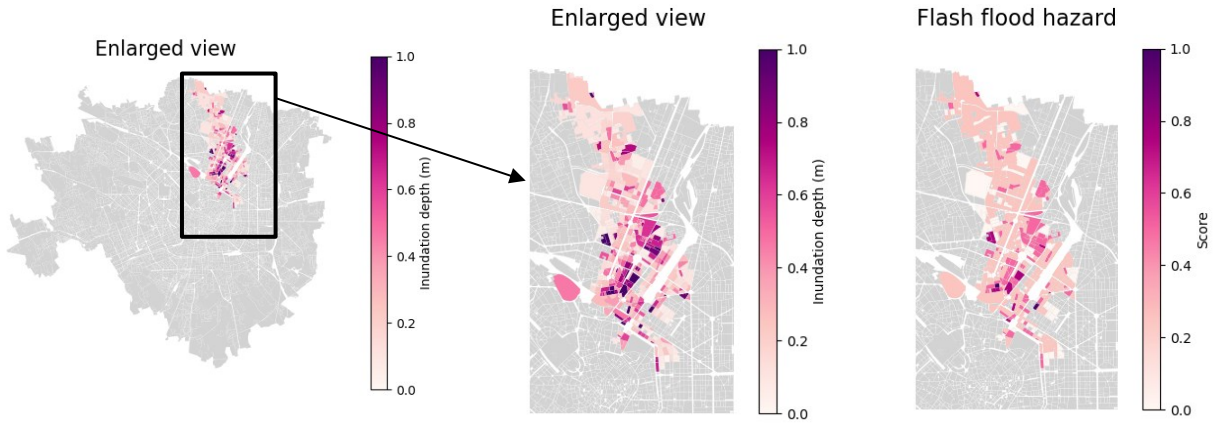

Figure 3. (a) Spatial variability of the mean inundation depth due to the Seveso river flash flood scenario with a 10-year mean return period, (b) enlarged view of the hazard scenario, and (c) flash flood hazard score.

Table 3. Hazard indicators, scores and weights for the peril of flash flooding in Milan, Italy.

Category	Indicator	Score	Weight	Reference
Intensity	Flood depth	Low (<0.1m): 0 Minor (0.1m to 0.5m): 0.25 Moderate (0.5m to 1m): 0.5 High (1m to 2m): 0.75 Extremely high (>2m): 1.0	1.0	Zischg et al. (2021); Leal et al. (2021)

3.5. Risk

Baseline assessment

The risk score is calculated according to Eq.(12) for each BB as the geometric mean of the three risk components scores and the spatial distribution of the risk scores for all BBs in the affected part of the city is presented in Figure 4a for the baseline assessment ("as is"). The identification of the most stressed parts of the city considering the existing COPs, corresponds to the so-called "baseline assessment" and can be further exploited, within the context of a first-level risk-aware DSS, for assisting decision makers to (a) direct their actions in those parts of the city that are needed most and (b) assess the efficiency of alternative mitigation measures in reducing the risk. The implementation of these measures/actions, which have been translated within the context of the proposed methodology into COP indicators, is expected to initially have an effect on the vulnerability score and ultimately on the risk score (risk mitigation scenario).

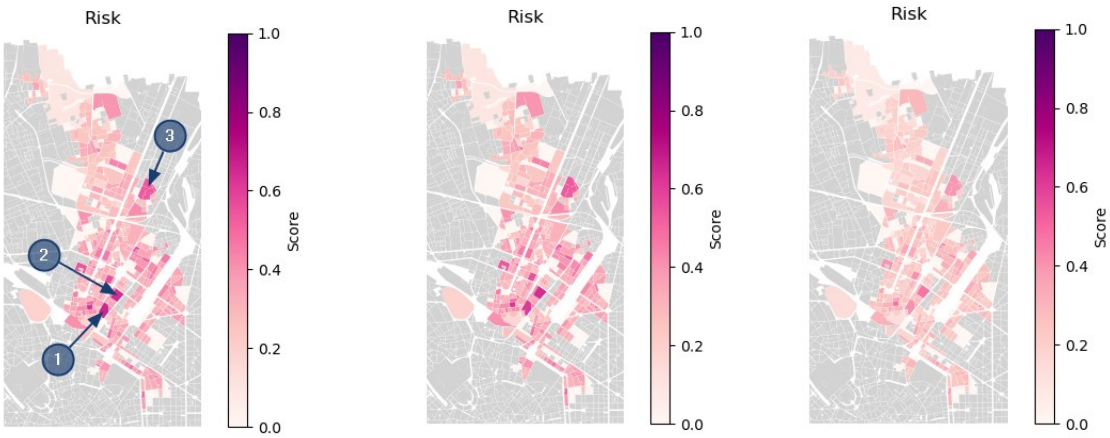

Figure 4. Risk scores for (a) the baseline assessment (and BB identification), (b) risk mitigation scenario 1, and (c) for risk mitigation scenario 2.

To demonstrate how the proposed methodology could be utilised in the context of a DSS for pre-event prioritisation of the risk mitigation actions, two risk mitigation scenarios will be examined hereafter. These scenarios will sequentially implement two mitigation measures, one with local and one with global (city/neighbourhood) scale effects. The mitigation measures will be implemented in addition to the already existing COPs in order to reduce the risk score in the most stresses areas of the city, as those were identified by the baseline assessment. Three BBs, i.e., BB1, BB2 and BB3 shown in Figure 4a, are selected and consequently analysed. The risk component scores and risk scores for the selected BBs are presented in Table 4.

Table 4. Vulnerability and risk assessment of the considered BBs. Scores before and after the implementation of two additional COPs.

	Hazard score			**Exposure score**			**Vulnerability score**			**Risk score**		
	BB1	**BB2**	**BB3**	**BB1**	**BB2**	**BB3**	**BB1**	**BB2**	**BB3**	**BB1**	**BB2**	**BB3**
Baseline assessment							0.37	0.35	0.34	0.66	0.64	0.56
Risk mitigation scenario 1: PG in BB1	0.75	0.75	0.5	1.0	1.0	1.0	0.30	0.35	0.34	0.61	0.64	0.56
Risk mitigation scenario 2: PG in BB1 and FPI							0.09	0.14	0.13	0.40	0.47	0.41

According to the baseline assessment (first row of Table 4), BB1 and BB2 present the highest risk scores, equal to 0.66 and 0.64, respectively, and vulnerability scores equal to 0.37 and 0.35, respectively, while BB3 possesses a vulnerability score that is comparable to those that are reported for BB1 and BB2, but it is associated with a lower risk score, i.e., 0.56, due to the lower hazard score in that particular BB. All three BBs have exposure scores that are equal to 1, i.e., the highest possible exposure score (essentially implying the presence of critical infrastructure).

Risk mitigation scenarios

In the first mitigation scenario (Risk mitigation scenario 1), the reduction of the risk score for BB1, which is the highest encountered among the considered BBs, is foreseen by implementing a local intervention measure. Local intervention measures primarily affect the BBs that are being implemented to and possibly neighbouring BBs (depending on the size and shape of the BBs), while they do not have any effect on distant BBs. Despite their restricted effect, local interventions usually require less time and resources compared to global ones and hence their implementation is deemed to be effective in regions that have only a few BBs with high risk scores and/or the available budget is limited. As such, PG COP is implemented in BB1 and the percentage of greenery of the referred BB is increased from 4.5% to 60%. The final/total percentage of greenery (i.e., 60%) is considered for the determination of the score of PG of BB1 for the mitigation scenario.

The effect of implementing PG in BB1 is reflected in both the vulnerability and the risk score of BB1, as shown in the second row of Table 4 (Risk mitigation scenario 1). The vulnerability score decreased from 0.37 to 0.30 (~19% reduction), while the risk score was reduced from 0.66 to 0.61 (~8% reduction). At the same time the vulnerability and risk scores in BB2 and BB3 remained, as expected, unaltered, since they are not within the 100 m radius that is likely to be affected by this COP. The risk scores of all BBs for the first risk mitigation scenario are illustrated in Figure 4b. It is important to note that due to the implementation of this mitigation measure, BB1 does not possess the maximum vulnerability and risk scores anymore. Instead, BB2 with vulnerability score equal to 0.35 and risk score equal to 0.64 (the same scores as in the baseline assessment) now possesses the highest scores. Furthermore, although the vulnerability score of BB1 due to the implementation of PG is lower than that of BB3 (vulnerability score of BB3 is 0.34, the same as in the baseline assessment), its risk score still remains higher than that of BB3 (risk score of BB3 is 0.56, the same as in the baseline assessment) due to the effect of the hazard component of the risk, which for BB1 receives a higher score compared to BB3 (i.e., BB1 is an area that is affected more by the considered flood hazard scenario compared to BB3).

In the second mitigation scenario (Risk mitigation scenario 2) an additional to the local PG mitigation measure is implemented, in an attempt to further reduce the risk. In particular, the construction of a FPI as per the latest design regulations, which a global scale intervention measure, is implemented in additional to the existing COPs and the local PG intervention that was implemented in BB1. The resulting vulnerability and risk scores after the implementation of this additional measure are presented in the third row of Table 4 (Risk mitigation scenario 2) for the three examined BBs, while the risk scores of all BBs are illustrated in Figure 4c. Contrary to the restricted in extent and the rather limited effect of PG, the implementation of FPI is seen to have a more significant effect on the risk scores of the BBs across the examined region. The latter observation was expected due to the higher weight that was attributed to this particular COP measure, and also due to the global character of this COP. It is thus observed that the vulnerability scores of BB2 and BB3 were reduced by 60% and ~62%, respectively, while the vulnerability score of BB1, which has the cumulative positive effect of both FPI and PG, was decreased by ~76% (with respect to the baseline assessment), reaching a value of only 0.09. As far as the risk scores are concerned, risk scores of both BB2 and BB3 dropped by ~27%, with BB2 still exhibiting the highest risk score, that however was reduced to a value that is lower than 0.5. The risk score of BB1, on the other hand, decreased by 34%, reaching a value of 0.40 that is even lower compared to that of BB3 (0.41), highlighting the effectiveness of implementing multiple COPs.

4. Final remarks

The proposed indicator-based vulnerability and risk assessment framework is a flexible and adjustable methodology, suitable for being implemented within a first-order risk-aware DSS that aims at serving the prioritisation of proactive actions against future hazardous events. It is mainly addressed to city authorities and urban planners and its purpose is to identify the most stressed areas of a city should a certain peril affects

them. Its formulation is generic and it can be utilised, with appropriate adjustments, for undertaking a vulnerability and risk assessment against a variety of perils in urban-scale applications.

The proposed methodology was demonstrated by considering the flash flood peril in the city of Milan, Italy. The presented case study was built upon a BB spatial resolution level, yet, subject to data availability, alternative, either more refined or coarser, spatial resolutions may be accommodated by the proposed framework. The vulnerability and risk scores of the baseline assessment were calculated and visualised in maps, highlighting the most stressed parts of the city under the considered flash flood scenario. Three BBs that presented the highest risk scores were further analysed and two alternative risk mitigation scenarios were consequently applied in order to examine the efficiency of the implemented coping capacity measures.

5. Acknowledgements

This research has received funding from the EU Horizon 2020 research and innovation programme HARMONIA, entitled “Development of a Support System for Improved Resilience and Sustainable Urban areas to cope with Climate Change and Extreme Events based on GEOSS and Advanced Modelling Tools” under agreement No. 101003517. The second author received funding by the UK Research and Innovation (UKRI) under the UK government’s Horizon Europe funding guarantee [Ref: EP/Y003586/1]. This is the funding guarantee for the European Union HORIZON-MSCA-2021-SE-01 [grant agreement No: 101086413] ReCharged - Climate-aware Resilience for Sustainable Critical and interdependent Infrastructure Systems enhanced by emerging Digital Technologies. The second author would also like to acknowledge funding by the UKRI under the UK government’s Horizon Europe funding guarantee [Ref: 10062091]. This is the funding guarantee for the European Union HORIZON-MISS-2021-CLIMA-02 [grant agreement No: 101093939] RISKADAPT - Asset-level modelling of risks in the face of climate-induced extreme events and adaptation. The authors would like to thank Christos Kontopoulos, Efthymios Magkoufis and Anna Papadima for providing the exposure data for the city of Milan and Jaakko Ikonen for providing the flash flood hazard. Special thanks also to Associate Prof. Dimitrios Vamvatsikos and Dr. Konstantinos Bakalis for the fruitful discussions during the development of the presented methodology.

6. References

Becciu G, Ghia M, Mambretti S (2018) A century of works on River Seveso: From unregulated development to basin reclamation. Int. J. Environ. Impacts, 1(4):461-472.

Bigi V, Comino E, Fontana M, Pezzoli A, Rosso M (2021) Flood vulnerability analysis in urban context: A socioeconomic sub-indicators overview. Climate, 9(1):12.

Birkmann J (2013) Measuring Vulnerability to Natural Hazards: towards disaster resilient societies (second edition), United Nations University Press.

Chang H, et al. (2021) Assessment of urban flood vulnerability using the social-ecological-technological systems framework in six US cities. Sustainable Cities Soc., 68, 102786.

Cutter SL, Boruff BJ, Shirley WL (2003) Social vulnerability to environmental hazards. Social science quarterly, 84(2):242-261.

Depietri Y, Dahal K, McPhearson T (2018) Multi-hazard risks in New York city. Nat. Hazards Earth Syst. Sci., 18(12):3363-3381.

Fuchs S, Birkmann J, Glade T (2012) Vulnerability assessment in natural hazard and risk analysis: current approaches and future challenges. Nat. Hazard., 64:1969-1975.

IPCC (2022a) Climate Change 2022: Impacts, Adaptation and Vulnerability. Contribution of Working Group II to the Sixth Assessment Report of the Intergovernmental Panel on Climate Change [H.-O. Pörtner, D.C. Roberts, M. Tignor, E.S. Poloczanska, K. Mintenbeck, A. Alegría, M. Craig, S. Langsdorf, S. Löschke, V. Möller, A. Okem, B. Rama (eds.)]. Cambridge University Press. Cambridge University Press, Cambridge, UK and New York, NY, USA, 3056 pp., https://doi.org/10.1017/9781009325844

IPCC (2022b) Annex I: Glossary [van Diemen, R., J.B.R. Matthews, V. Möller, J.S. Fuglestvedt, V. Masson-Delmotte, C. Méndez, A. Reisinger, S. Semenov (eds)]. In IPCC, 2022: Climate Change 2022: Mitigation of Climate Change. Contribution of Working Group III to the Sixth Assessment Report of the Intergovernmental Panel on Climate Change [P.R. Shukla, J. Skea, R. Slade, A. Al Khourdajie, R. van Diemen, D. McCollum, M. Pathak, S. Some, P. Vyas, R. Fradera, M.

Kappes MS, Papathoma-Kohle M, Keiiler M (2012) Assessing physical vulnerability for multi-hazards using an indicator-based methodology. Appl. Geogr., 32(2): 577−590.

Karagiorgos K, Thaler T, Hübl J, Maris F, Fuchs S (2016) Multi-vulnerability analysis for flash flood risk management. Nat. Hazard., 82, 63-87. https://doi.org/10.1007/s11069-016-2296-y

Kim H, Lee DK, Sung S (2016) Effect of urban green spaces and flooded area type on flooding probability. Sustainability, 8(2), 134.

Kontopoulos C, Magkoufis E, Papadima A, Skoulidou D, Kazantzi A, Hafner S (2023) A novel web-based decision support tool for enhancing urban resilience and sustainability. 9th International Conference on Remore Sensing and Geoinformation of Environment, Cyprus.

Krellenberg K, Welz J (2017) Assessing urban vulnerability in the context of flood and heat hazard: Pathways and challenges for indicator-based analysis. Social Indic. Res., 132, 709-731.

Leal M, Reis E, Pereira S, Santos PP (2021) Physical vulnerability assessment to flash floods using an indicator-based methodology based on building properties and flow parameters. J. Flood Risk Manage., 14(3):e12712. https://doi.org/10.1111/jfr3.12712

Mitoulis SA, Bompa DV, Argyroudis S (2023) Sustainability and climate resilience metrics and trade-offs in transport infrastructure asset recovery. Transp Res D Transp Environ, 121, 103800.

Moreira LL, de Brito MM, Kobiyama M (2021) A systematic review and future prospects of flood vulnerability indices. Nat. Hazards Earth Syst. Sci., 21(5):1513-1530.

Muller A, Reiter J, Weiland U (2011) Assessment of urban vulnerability towards floods using an indicator-based approach–a case study for Santiago de Chile. Nat. Hazards Earth Syst. Sci., 11(8):2107-2123.

Papathoma-Kohle M, Cristofari G, Wenk M, Fuchs S (2019) The importance of indicator weights for vulnerability indices and implications for decision making in disaster management. Int. J. Disaster Risk Reduct., 36:101103. https://doi.org/10.1016/j.ijdrr.2019.101103

Papathoma-Kohle M, Schlögl M, Dosser L, Roesch F, Borga M, Erlicher M, Keiler M, Fuchs S (2022) Physical vulnerability to dynamic flooding: Vulnerability curves and vulnerability indices. J. Hydrol. 607, 127501.

Pathak S, Panta HK, Bhandari T, Paudel KP (2020) Flood vulnerability and its influencing factors. Nat. Hazard., 104, 2175-2196.

Rasanen A, Heikkinen K, Piila N, Juhola S (2019) Zoning and weighting in urban heat island vulnerability and risk mapping in Helsinki, Finland. Reg. Environ. Change, 19, 1481-1493.

Ravazzani G, Amengual A, Ceppi a, Homar V, Romero R, Lombardi G, Mancini M (2016) Potentialities of ensemble strategies for flood forecasting over the Milano urban area. J. Hydrol., 539: 237−253.

Taramelli A, Righini M, Valentini E, Alfieri L, Gatti I, Gabellani S (2022) Building-scale flood loss estimation through vulnerability pattern characterization: application to an urban flood in Milan, Italy. Nat. Hazards Earth Syst. Sci., 22(11), 3543-3569.

Thouret JC, Ettinger S, Guitton M, Santoni O, Magill C, Martelli K, Zuccaro G, Revilla V, Charca JA, Arguedas A (2014) Assessing physical vulnerability in large cities exposed to flash floods and debris flows: the case of Arequipa (Peru). Nat. Hazard., 73, 1771-1815.

UNISDR (United Nations International Strategy for Disaster Reduction) (2015) Sendai framework for disaster risk reduction 2015–2030. Geneva: UNISDR.

World Bank, World Development Indicators (2023a) Population ages 0-14 (% of total population) – European Union. Retrieved from https://data.worldbank.org/indicator/SP.POP.0014.TO.ZS. Accessed 13/06/23.

World Bank, World Development Indicators (2023b) Population ages 65 and above (% of total population) – European Union. Retrieved from https://data.worldbank.org/indicator/SP.POP.65UP.TO.ZS. Accessed 13/06/23.

World Bank, World Development Indicators (2023c) Unemployment, total (% of total labor force) (national estimate) – European Union. Retrieved from https://data.worldbank.org/indicator/SL.UEM.TOTL.NE.ZS. Last accessed: June, 13th, 2023.

Zischg AP, Röthlisberger V, Mosimann M, Profico-Kaltenrieder R, N Bresch D, Fuchs S, Kauzlaric M, Keiler M (2021) Evaluating targeted heuristics for vulnerability assessment in flood impact model chains. J. Flood Risk Manage., 14(4), e12736. https://doi.org/10.1111/jfr3.12736